Luminescence Studies of Perturbation of Tryptophan Residues of Tubulin in the Complexes of Tubulin with Colchicine and Colchicine Analogues†

Pinki Saha Sardar,‡ Shyam Sundar Maity,‡ Lalita Das,§ and Sanjib Ghosh*,‡

Department of Chemistry, Presidency College, Kolkata 700 073, India, and Department of Biochemistry, Bose Institute, Kolkata 700 054, India

Received July 18, 2007; Revised Manuscript Received October 8, 2007

ABSTRACT: Tubulin, a heterodimeric ($\alpha\beta$) protein, the main constituent of microtubules, binds efficiently with colchicine (consisting of a trimethoxybenzene ring, a seven-member ring and methoxy tropone moiety) and its analogues, viz., demecolcine and AC [2-methoxy-5-(2′,3′,4′-trimethoxyphenyl)tropone]. Tubulin contains eight tryptophan (Trp) residues at A21, A346, A388, A407, B21, B103, B346, and B407 in the two subunits. The role of these eight Trp residues in this interaction and also their perturbation due to binding have been explored via time-resolved fluorescence at room temperature and low-temperature (77 K) phosphorescence in a suitable cryosolvent. Both the time-resolved fluorescence data and 77 K phosphorescence spectra indicate that the emitting residues move toward a more hydrophobic and less polar environment after complex formation. The environment of emitting Trps in the complex also becomes slightly more heterogeneous. Our analysis using the experimental results, the calculation of the accessible surface area (ASA) of all the Trps in the wild type and tubulin−colchicine complex [Ravelli, R. B. G., et al. (2004) *Nature 428*, 198−202], the distance of the Trp residues from the different moieties of the colchicine molecule, the knowledge of the nature of the immediate residues (<5 Å) present near each Trp residue, and the calculation of the intramolecular Trp−Trp energy transfer efficiencies indicate that Trp A346, Trp A407, Trp B21, and Trp B407 are the major contributors to the emission in the free protein, while Trp B21 and Trp B103 are mainly responsible for the emission of the complexes. A comparative account of the photophysical aspects of the drug molecules bound to protein in aqueous buffer and in buffer containing 40% ethylene glycol has been presented. The quantum yield and average lifetime of fluorescence in tubulin and its complexes with colchicine are used to predict the possible donors and the energy transfer (ET) efficiency in the ET process from Trps to colchicine in the complex. This study is a unique attempt to identify the Trp residues contributing to the emission in the free protein and in a complex of a multi-Trp protein with a drug molecule without performing the mutation of the protein.

The microtubules found in eukaryotic organisms are responsible for a variety of functions, including cell division, intracellular transport and secretion processes, ciliary and flagellar movement, morphogenesis, and cell orientation (*1*, *2*). The microtubules are largely composed of tubulin, a heterodimeric ($\alpha\beta$) protein with a molecular mass of 110 000 kDa (*3*), and the two chains, α and β, have very similar amino acid compositions. One of the most characteristic properties of tubulin is its ability to bind the plant alkaloid, colchicine. Colchicine (Figure 1), obtained from *Colchicum autmnale* and *Gloriosa superba*, is used in the treatment of autoinflammatory diseases and gout. Colchicine has anti-inflammatory, anti-mitotic, and anti-fibrotic activity (*4*). Colchicine also finds applications in various other diseases like pseudogout, familial Mediterrenian fever, cirrhosis of the liver and bile, and amyloidosis (*5*, *6*). Colchicine and colchicine-site binding agents have been widely used as probes to understand the properties and functions of microtubules in cells. Initially, tubulin was purified on the basis of its high affinity for colchicine. In plants, colchicine is widely used to separate chromosomes at the metaphase and

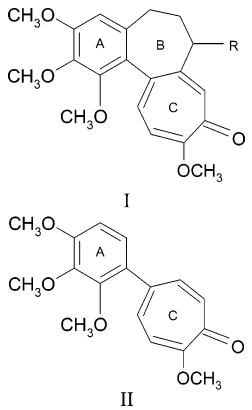

FIGURE 1: Structure of colchicine (I) (R = $NHCOCH_3$) and B ring analogues of colchicine (for damacolchicine, R = $NHCOCH_2SH$; for colcemid, R = $NHCH_3$) and structure of AC (II).

† This work was financially supported by the Department of Science and Technology (DST), Government of India (Grants SP/S1/PC-34/2002 and SR/S5/NM-14/2003), and by the Council of Scientific and Industrial Research, Government of India [Grant 01(2142)/07/EMR-II].

* To whom correspondence should be addressed: Department of Chemistry, Presidency College, 86/1, College Street, Kolkata 700 073, India. Telephone: +91-033-22413893. Fax: +91-033-22412738. E-mail: sanjibg@cal2.vsnl.net.in.

‡ Presidency College.

§ Bose Institute.

10.1021/bi701412k CCC: $37.00
Published on Web 11/28/2007

to induce polyploidy (*7*). Recently, colchicine has been used as a selective neurotoxin in animal models to study Alzheimer's dementia (*8*, *9*). It consists of three rings, namely, ring A (trimethoxybenzene ring), seven-member ring B, and ring C (the methoxytropone moiety), with a side chain on the C-7 position of ring B (Figure 1). Colchicine inhibits tubulin polymerization and in a substoichiometric amount affects tubulin−microtubule dynamics (*10*, *11*), but its use, as a potential anticancer agent, has been restricted due to its neurotoxicity (*12*, *13*).

The colchicine molecule which is nonfluorescent in the free state in aqueous medium fluoresces after binding to tubulin around 430 nm (*14*). The binding site of colchicine on tubulin has been recently defined from the crystal structure of the tubulin−damacolchicine complex at 3.58 Å resolution (*15*). From the crystal structure, it has been observed that the colchicine site is mostly buried in the intermediate domain of the β subunit, while the B ring side chain of colchicine interacts with the α subunit. Tubulin consists of eight tryptophan residues; each subunit contains four of each (A21, A346, A388, and A407 in the α subunit and B21, B103, B346, and B407 in the β subunit).

The tubulin−colchicine binding was examined by Bhattacharyya and Wolff (*16*) on the basis of the fluorescence study, where it was observed that the binding of colchicine leads to significant quenching of Trp fluorescence and simultaneous marked enhancement of colchicine fluorescence when excited at the absorption peak (353 nm) of colchicine in PEM buffer (pH 7) [quantum yield (ϕ) = 0.03] (*16*). The investigation of the binding of colchicine has revealed that the colchicine binds to a single site on the tubulin dimer, substoichiometrically inhibiting its assembly into microtubules both in vitro and in vivo (*17*−*20*) slowly and almost irreversibly (*17*, *21*). The fluorescence studies emphasized that at least two moieties of the colchicine are involved in binding (*16*). One is ring A or the trimethoxyphenyl ring, and the other is ring C, methoxytropone ring. Detrich et al.'s (*22*) recent work reported that the negative CD band of the colchicine chromophore at 340 nm vanishes when colchicine is bound to tubulin. This was supported by the fact there was more than one conformation of the colchicine molecule, and a conformational change was responsible during binding with tubulin. The change in conformation 1 to conformation 2 (a nearly planar structure of the unsaturated moieties exhibiting extended conjugation induced by protein binding) might be responsible for the enhanced fluorescence of colchicine (*16*, *22*). The kinetics of the colchicine−tubulin interaction were also established by monitoring the induction of the colchicine fluorescence (*23*, *24*).

The binding interaction of tubulin was also established by the various congeners or B ring analogues of colchicine, namely, colcemid (or demecolcine) and AC[1] [2-methoxy-5-(2′,3′,4′-trimethoxyphenyl)tropone] in many published works (*17*, *21*, *22*, *25*, *26*). Unlike colchicine, these model compounds bind tubulin very rapidly and reversibly, though induction of fluorescence is more prominent in the case for AC, whereas colcemid remains nonfluorescent after binding. The facile rotation about the biaryl bond to adopt a more planar bound conformation is responsible for promotion of fluorescence which is impossible for the colcemid−tubulin complex due to the unfavorable conformation (*23*, *27*, *28*). The work on binding of drugs with tubulin was also established by considering the activity of the B ring, which shows a major role for studying thermodynamic and kinetic parameters (*26*, *29*, *30*). A red edge excitation shift (REES) study (*31*) on the Trp fluorescence of tubulin and its complexes with colchicine and colchicine analogues revealed that the average Trp environment in tubulin is motionally restricted and also the tryptophan(s) participating in energy transfer with bound colchicine probably does not contribute to the REES (*31*, *32*).

One of the purposes of using intrinsic tryptophan luminescence as a probe for protein structure, dynamics, and function is to assign the spectral contribution to individual Trp residues when a protein contains more than one Trp residue (*33*). Characterization of Trp residue in a protein or protein−drug complex using steady state and time-resolved fluorescence of the Trp residues is not always unambiguous since the fluorescence spectra of Trp residues are always broad and the lifetime of fluorescence even in a protein containing a single Trp residue exhibits a multiexponential decay. On the other hand, phosphorescence spectra of Trp residues in proteins at a low temperature (77 K) (LTP) in a suitable cryosolvent always give structured spectra with definite (0,0) band characteristics of the Trp environment (*34*−*38*). Several cases in which multi-tryptophan proteins give rise to more than one (0,0) band corresponding to different Trp residues indicating inefficient photoinduced energy transfer between Trp residues have also been reported (*39*). The narrowness of the LTP bands, in contrast with the poorly resolved fluorescence of tryptophan, is attributed to the smaller excited state dipole moment in the case of the lowest excited triplet state (*39*). The LTP of the tryptophan residues buried in hydrophobic regions within proteins is generally red-shifted relative to solvent-exposed residues, and it is better resolved since buried environments are usually more highly structured, i.e., homogeneous (*40*). Specific interactions with polar residues, however, can result in blue-shifted origins for buried Trp residues (*41*, *42*). Thus, investigation using time-resolved fluorescence along with low-temperature phosphorescence often provides a meaningful and unambiguous interpretation (*37*, *38*).

In this work, we characterize the interaction of the colchicine and its analogues, namely, colcemid and AC, with the tubulin molecule by time-resolved fluorescence and low-temperature (77 K) phosphorescence studies in a suitable cryosolvent to ascertain the involvement and the perturbation of Trp residues in both the α and β subunits of tubulin in the complexed state. The calculation of accessible surface area (ASA), the distances of the Trp residues from rings A, B, and C of colchicine, and the knowledge of the nature of immediate residues (within 5 Å) of eight Trp residues in the free protein and in the complex are utilized to interpret the results. Furthermore, the calculation of singlet−singlet intramolecular energy transfer efficiencies among the eight tryptophan residues aids in our understanding of the contribution of individual Trp residues to the emission of the free protein and the complex. This study presents a unique model for ascertaining the role of a particular Trp residue(s) in the

[1] Abbreviations: PIPES, piperazine-*N*,*N*′-bis(2-ethanesulfonic acid); EGTA, ethylene glycol bis(β-aminoethyl ether)-*N*,*N*,*N*′,*N*′-tetraacetic acid; GTP, guanosine 5′-triphosphate; DMSO, dimethyl sulfoxide; LTP, low-temperature phosphorescence; AC, 2-methoxy-5-(2′,3′,4′-trimethoxyphenyl)tropone; PDB, Protein Data Bank; ASA, accessible surface area; ET, energy transfer; EG, ethylene glycol.

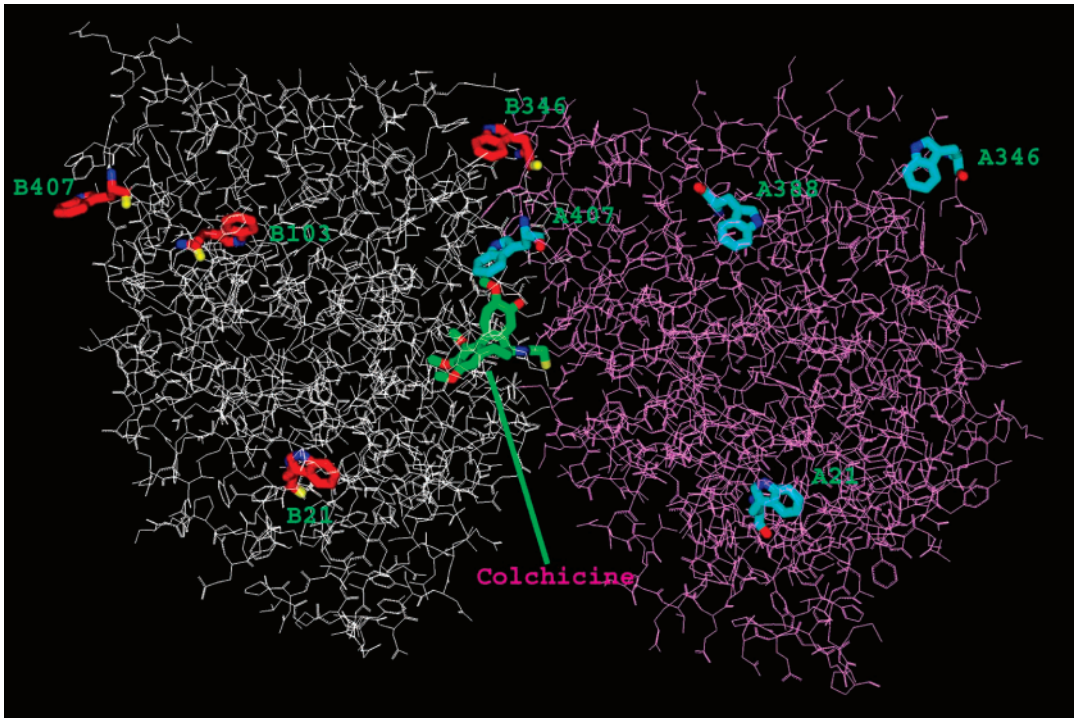

FIGURE 2: Structure of α (in wire representation in pink) and *β* (in wire representation in white) subunits of colchicine-bound tubulin (PDB entry 1SA0). Four tryptophan residues of each subunit are shown in stick form with different colors (*β* in red and α in cyan). The colchicine molecule is depicted as a stick representation in green.

protein−drug interaction without using the Trp mutated proteins (*43*).

EXPERIMENTAL PROCEDURES

Materials. Demecolcine was purchased from Sigma. Colchicine and the other colchicine analogue AC, piperazine-*N*,N′-bis(2-ethanesulfonic acid) (PIPES), ethylene glycol bis-(*β*-aminoethyl ether)-*N*,*N*,*N*′,*N*′-tetraacetic acid (EGTA), guanosine 5′-triphosphate (GTP), and magnesium chloride ($MgCl_2$) were kindly supplied by B. Bhattacharyya of Bose Institute (Calcutta, India). Ethylene glycol was purchased from Alfa Aeiser. Other reagents were of analytical grade.

Drugs. The stock solution of colchicine was made in water, and the stock solutions of the demecolcine and AC were prepared in 100% DMSO and their concentrations determined spectrophotometrically by use of an extinction coefficient in water ($\epsilon = 16\,790\ M^{-1}\ cm^{-1}$ for colchicine at 353 nm, $\epsilon = 15\,800\ M^{-1}\ cm^{-1}$ for demecolcine at 354 nm, and $\epsilon = 18\,840\ M^{-1}\ cm^{-1}$ for AC at 341 nm).

Tubulin Isolation and Estimation. Microtubular proteins were isolated from goat brains by two cycles of a temperature-dependent assembly−disassembly process. Pure tubulin was isolated from microtubular proteins by two additional cycles of temperature-dependent polymerization and depolymerization using 1 M glutamate buffer for assembly (*44*). The assembly buffer (PEM buffer) consisted of 50 mM PIPES (pH 6.9), 1 mM EGTA, 0.5 mM $MgCl_2$, and 0.5 mM GTP. The protein was stored at −70 °C. The protein concentration was determined by the method of Lowry et al. (*45*) using bovine serum albumin as a standard.

Modeling of the Tubulin−Drug Complex. The model of the tubulin−drug complex was generated from the crystal structure of the damacolchicine-bound tubulin complexed with stathmin-like domain (PDB entry 1SA0) (damacolchicine is a side chain analogue of colchicine) (Figure 2) (*15*). The coordinates corresponding to one tubulin dimer bound to damacolchicine were removed. The damacolchicine molecule was replaced with colchicine (side chain replaced by $NHCOCH_3$), colcemid (side chain replaced by NHMe), or AC. The resultant modeled complexes were subjected to energy minimization using the steepest decent method followed by a conjugate gradient in the BIOSYM module of INSIGHT II (Biosym/MSI, 1995).

Calculation of Accessible Surface Area. The surface area for the free protein was calculated from the *αβ* tubulin dimer fitted to a 3.7 Å density map obtained by electron crystallography of zinc-induced tubulin sheets (PDB entry 1TUB) (*46*). The ASA values were calculated using NACCESS designed by S. J. Hubbard and J. M. Thornton (*47*).

INSTRUMENTATION

UV−visible absorption spectra were recorded on a Hitachi U-3210 spectrophotometer at 298 K. The steady state fluorescence measurements were carried out in a Hitachi F-4010 spectrofluorimeter (equipped with a 150 W xenon lamp) using a 1 cm path length quartz cuvette. All the measurements at 298 K were taken by exciting the samples at 280 and 295 nm using 5 nm band-passes for excitation and emission using the correct mode of the instrument. Inner filter effects have been eliminated in all the emission spectra.

The fluorescence quantum yield (*ϕ*) is determined in each case by comparing the corrected emission spectrum of the samples with that of tryptophan in water ($\phi_D = 0.14$) (*48*, *49*) considering the total area under the emission curve.

Emission studies at 77 K were conducted using a Dewar system having a 5 mm outside diameter quartz tube. Freezing of the samples at 77 K was carried out at the same rate for

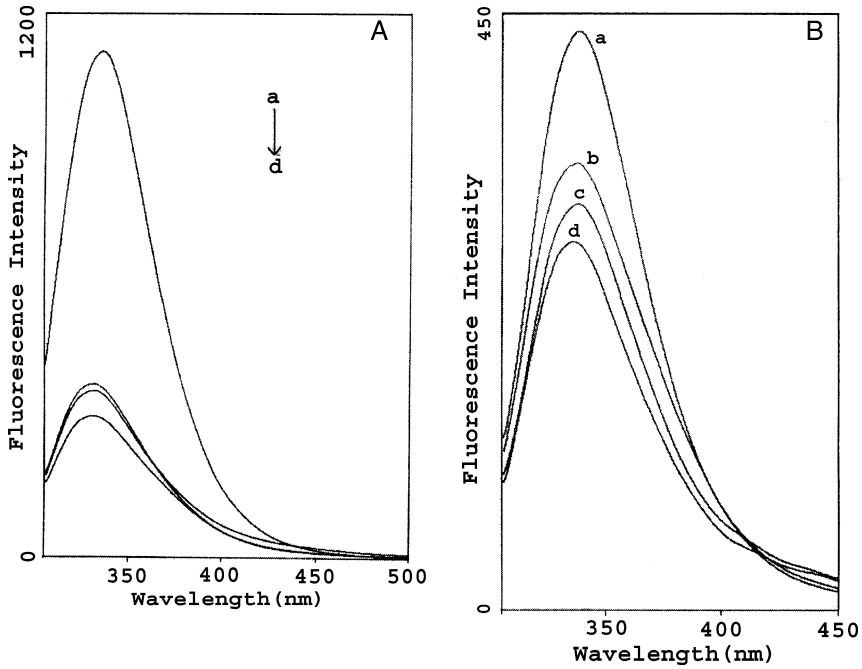

FIGURE 3: (A) Corrected fluorescence spectra of wild-type tubulin (2 μM) and its complexes with different drugs in PEM buffer at 298 K: (a) wild-type tubulin, (b) tubulin with colcemid, (c) tubulin with colchicine, and (d) tubulin with AC. The concentration of the drug was 10 μM in each case. The excitation wavelength was 295 nm. Excitation and emission band-passes were 5 nm each. (B) Corrected fluorescence spectra of wild-type tubulin (2 μM) and its complexes with different drugs in PEM buffer containing 40% ethylene glycol at 298 K: (a) wild-type tubulin, (b) tubulin with colcemid, (c) tubulin with colchicine, and (d) tubulin with AC. The concentration of the drug was 10 μM in each case. The excitation wavelength was 295 nm. Excitation and emission band-passes were 5 nm each.

all the samples. Triplet state emissions were measured in a Hitachi F-4010 spectrofluorimeter equipped with phosphorescence accessories at 77 K. All the samples were made in 40% ethylene glycol for low-temperature measurements. The samples were excited at 295 nm using a 10 nm band-pass, and the emission band-pass was 1.5 nm. The cryosolvent (40% ethylene glycol) used in the experiment was always found to form a clear glass. The low-temperature (77 K) spectra were found to be reproducible and free from any polarization artifacts. We have checked the low-temperature spectra using magic angle polarizer conditions (the excitation polarizer is oriented in the vertical position, and the emission polarizer is oriented 54.7° from the vertical) for standard samples such as bovine serum albumin (BSA) and horse liver alcohol dehydrogenase (HLAD).

Singlet state lifetimes were measured with a Time Master fluorimeter from Photon Technology International (PTI). The system measures the fluorescence lifetime using PTI's patented strobe technique and gated detection. Felix 32 controls all acquisition modes and data analysis of the Time Master system. The sample was excited using a thyratron-gated nitrogen flash lamp (full width at half-maximum of 1.2 ns) that is capable of measuring fluorescence time-resolved acquisition at a flash rate of 25 kHz as well as with Nano-LED (295 nm) (full width at half-maximum of 1.0 ns). Lamp profiles were measured at the respective excitation wavelengths, viz., 297 and 337 nm (in the case of the nitrogen flash lamp) and 295 nm (in case of LED), using slits with a band-pass of 3 nm using Ludox as the scatterer. The decay of protein samples was recovered using Nano-LED (295 nm), and for the drug emission, the 337 nm nitrogen flash lamps were used in a nonlinear iterative fitting procedure based on the Marquardt algorithm. A deconvolution technique can determine the lifetime up to 300 ps with Nano-LED. The quality of the fit has been assessed over the entire decay, including the rising edge, and tested with a plot of weighted residuals and other statistical parameters, e.g., the reduced χ^2 ratio and the Durbin−Watson (DW) parameters. The phosphorescence lifetime was measured using a Hitachi F-4010 spectrofluorimeter equipped with a phosphorescence accessory.

RESULTS AND DISCUSSION

Steady State Fluorescence Studies at 298 K. Bhattacharyya et al. (*16*) reported that colchicine is nonfluorescent in PEM buffer when excited at the absorption peak (353 nm) of colchicine. When tubulin and colchicine are incubated together at 37 °C, fluorescence from the colchicine is observed with an emission maximum at 430 nm using a λ_{exc} of 350 nm. The binding of colchicine also leads to quenching of Trp fluorescence on excitation at 295 nm due to formation of the complex (*27*, *32*). Later work (*26*, *27*, *29*, *30*) with analogues of colchicine (colcemid and AC) also revealed similar behavior of the fluorescence of the protein and the complexes.

In this work, steady state fluorescence studies at 298 K of wild-type tubulin (2 μM, pH 7) and the complex of tubulin with colchicine, colcemid, and AC (10μM) have been carried out in PEM buffer and in PEM buffer containing 40% EG (henceforth PEM buffer in 40% EG will be termed 40% EG) with excitation at 280 and 295 nm. The emission spectra show that the emission maximum of tubulin is slightly blue-shifted in all the complexes compared to that of free tubulin for both the excitations (Figure 3A,B and Table 1) in both aqueous buffer and 40% EG. The quantum yields of fluorescence of wild-type tubulin and the complexes with all three drug molecules in PEM buffer are given in Table 1.

Table 1: Fluorescence Data for Wild-Type Tubulin (2 μM) and Its Complexes with Different Drugs (10 μM) in PEM Buffer and in 40% EG at 298 K

system	λ_{exc} (nm)	λ_{max} of emission in PEM buffer (nm)[a]	λ_{max} of emission in 40% EG (nm)[a]	quantum fluorescence yield in PEM buffer[b]
wild-type tubulin	280	336.8	337.4	–
	295	337.8	338.6	0.060
tubulin with colchicine	280	333.4	333.2	–
	295	336.4	335.4	0.025
tubulin with colcemid	280	334.8	334.2	–
	295	336.8	337.6	0.026
tubulin with AC	280	335.6	335.4	–
	295	336.8	335.8	0.018

[a] Error in the measurement of $\pm$0.4 nm. [b] The intensities are calculated in each case using the total area under the respective band.

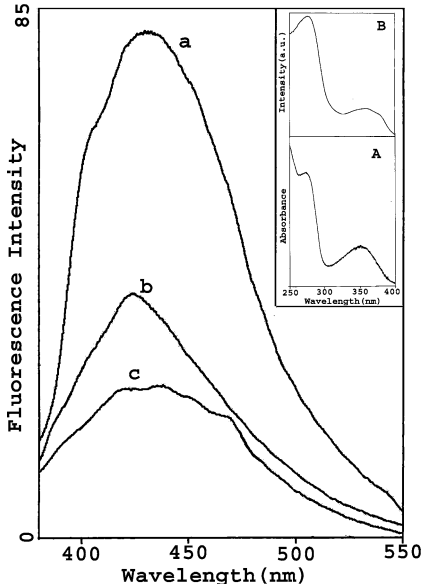

FIGURE 4: Fluorescence spectra of complexes of tubulin (2 μM) with different drugs in PEM buffer at 298 K: (a) tubulin with colchicine, (b) tubulin with AC, and (c) tubulin with colcemid. The concentration of the drug was 10 μM in each case. The excitation wavelength was 340 nm. Excitation and emission band-passes were 5 nm each. In the inset are (A) the absorption spectrum and (B) the excitation spectrum derived by monitoring colchicine fluorescence at 430 nm of the tubulin (2 μM)–colchicine (10 μM) complex. Excitation and emission band-passes were 5 nm each.

Figures 4 and 5 show the fluorescence of three drug molecules bound to tubulin in PEM buffer and in 40% EG, respectively, at a λ_{exc} of 350 nm. The absorption spectra of the colchicine complex and the excitation spectra in PEM buffer during monitoring of the drug emission at 430 nm are shown in the inset of Figure 4. Previous work of Bhattacharyya (*50*) established that in a highly viscous medium (glycerol) colchicine exhibits fluorescence. However, the enhancement is smaller than that of bound colchicine in aqueous buffer. In this study, we carried out a comparative account of drug fluorescence enhancement of tubulin–drug complexes in 40% EG and in PEM buffer (Table 2). Bound drugs exhibit ~2–3 times more intense fluorescence in 40% EG than bound drugs in PEM buffer (Table 2). It is also noted that the emission of the drugs in the complexes in a 40% EG matrix is more structured than

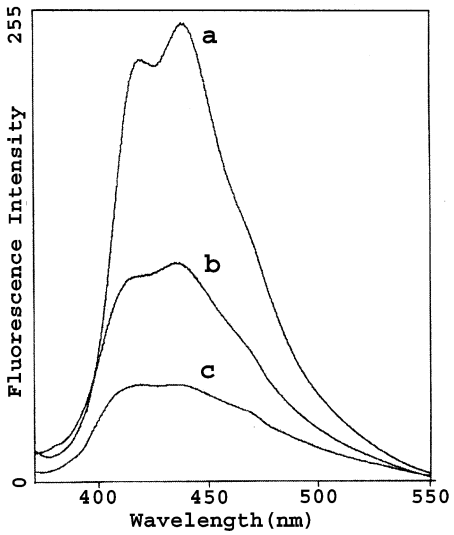

FIGURE 5: Fluorescence spectra of complexes of tubulin (2 μM) with different drugs in PEM buffer containing 40% ethylene glycol at 298 K: (a) tubulin with colchicine, (b) tubulin with colcemid, and (c) tubulin with AC. The concentration of the drug was 10 μM in each case. The excitation wavelength was 340 nm. Excitation and emission band-passes were 5 nm each.

Table 2: Comparison of Enhancement of Drug Fluorescence at 298 K

system	ratio of the drug fluorescence in tubulin–drug complexes in 40% EG to that in PEM buffer[a]	ratio of the drug fluorescence in tubulin–drug complexes in 40% EG matrix to that of the free drug molecules in 40% EG matrix
tubulin–colchicine	2.2	14.5
tubulin–colcemid	2.8	6.5
tubulin–AC	2.0	3.5

[a] The intensities are calculated in each case using the total area under the respective band.

those in aqueous buffer (Figure 5). We observed that the emission of colchicine bound to tubulin in 40% EG is enhanced to a maximum extent (enhancement factor of 14.5) compared to that of free colchicine in 40% EG. For the other drug molecules, colcemid and AC, the enhancement factors are 6.5 and 3.5, respectively (Table 2).

Time-Resolved Fluorescence Studies at 298 K. Panels A and B of Figure 6 show the time-resolved fluorescence decay at 298 K for both wild-type tubulin and tubulin–drug complexes in PEM buffer and 40% ethylene glycol captured by monitoring the protein emission maxima (Table 3). The decays were best fitted with two components where χ^2 is found to be close to 1 in each case (Figure 6A,B and Table 3). Attempts to fit the data with three or four components resulted in greater χ^2 values. In aqueous buffer medium, the longer components of 4.7 ns contribute 21% whereas the shorter component of ~1 ns is the major component with a 79% contribution (Table 3). The data agreed well with those reported by Guha et al. (*31*).

Interpretations of complex decay of tryptophan fluorescence fall into two main categories: ground state heterogeneity (e.g., rotamer model) and excited state reaction (e.g., relaxation model). Proteins, in contrast, are heterogeneous

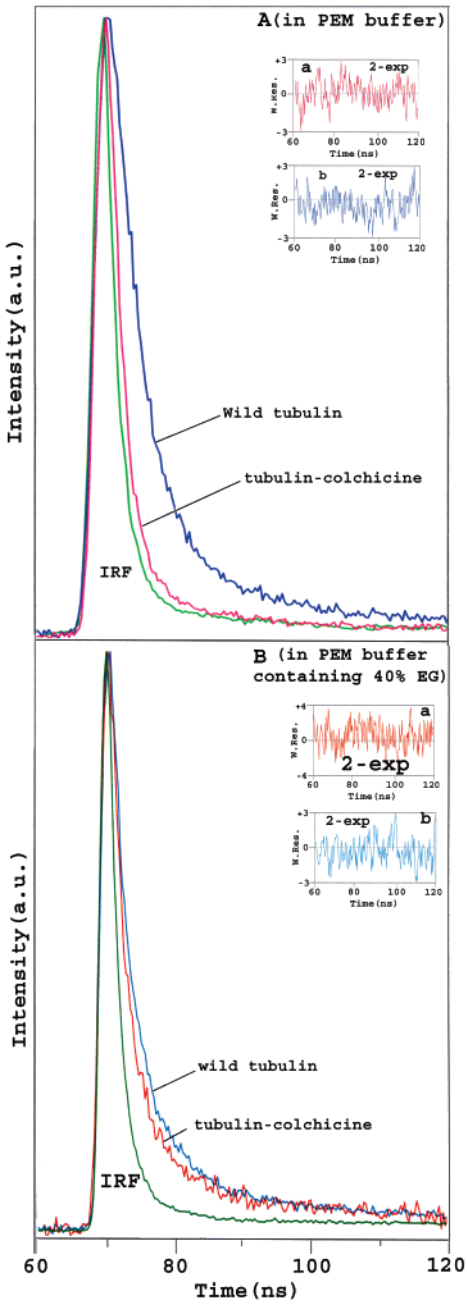

FIGURE 6: Fluorescence decay of wild-type tubulin (2 μM) and tubulin (2 μM) with colchicine (10 μM) in (A) PEM buffer and (B) PEM buffer containing 40% EG at 298 K (λ_{exc} = 297 nm, $\lambda_{monitor}$ = 335 nm; excitation band-pass = 15 nm, emission band-pass = 10 nm).

systems with a hierarchy of internal motions that cover a wide range of correlation times, including the nanosecond time window of fluorescence. However, the excited state reaction approach relies on protein dynamics for conversion of electronically excited indole into other spectroscopic species. More specifically, the relaxation model assumes that such a reaction involves reorientation of polar groups surrounding tryptophan in a protein (*51*−*53*). Neither of the models has been unequivocally proven for any specific protein.

In all the complexes, we found that the longer component becomes somewhat shorter (3.5−4.0 ns) with a less than 20% contribution, whereas the shorter component of 1 ns observed in the free protein is much shortened (~0.4 ns) with a slightly greater than 80% contribution. The average lifetime decreases from 1.8 ns in the free proteins to 1 ns in all the complexes in PEM buffer. The lifetime data for the complexes definitely suggest that Trp residues in tubulin are perturbed due to complex formation. Specifically, the reduction of the 1 ns component in the free proteins to ~0.4 ns in the complexes indicates that the emission arises from a blue-shifted Trp in a comparatively buried environment (*54*−*59*) (see also the next section).

In a 40% EG matrix, the lifetime values follow a similar trend. However, the components have longer lifetimes (Table 3). The average lifetime of 2.2 ns in the wild-type protein is reduced to 1.8 ns in the complexes. The longer component of ~5.9 ns with a 10% contribution becomes 5.5 ns with a more or less similar contribution in the complexes. The shorter component (1.5 ns) is reduced to 1.2−1.3 ns in the complexes. These results again imply that the major emitting residue(s) moves toward a comparatively more buried region after complex formation.

The lifetime of the drugs around 430 nm (using λ_{exc} = 337 nm) is found to fit with a single exponential with τ values of 0.9−1.1 ns (Table 3 and Figure 7), which agrees exactly with the reported results (*31*, *60*) for colchicine. The agreement lends support to our other measurements mentioned earlier. It is noted that the lifetime of the drug emission in the presence of tubulin remains unaltered when the medium is changed from PEM buffer to 40% EG. The quantum yield of the drug emission in the complexes is greater in a 40% EG matrix than in buffer (Table 2). The results imply that the radiative rate (k_r) is enhanced with a simultaneous decrease in the nonradiative rate (k_{nr}) in 40% EG.

Phosphorescence Study. The phosphorescence spectra of the wild-type tubulin and its complexes with the three drug molecules, colchicine, AC, and colcemid, with a λ_{exc} of 295 nm in a 40% ethylene glycol matrix at 77 K show a single (0,0) band (Figure 8). The (0,0) band of wild-type tubulin appears at 407.6 nm, while the (0,0) bands of the three complexes of the protein occur at 412.0, 412.0, and 412.2 nm, respectively (Figure 8 and Table 4). The bandwidths (obtained by using a curve fitting procedure) (*37*, *38*) of the (0,0) bands of the free protein and the complexes with the drug molecules are also calculated and given in Table 4.

Proteins containing more than one Trp residue generally exhibit a single (0,0) band in their phosphorescence spectra. The quenching of phosphorescence from other Trp residues may be due to (i) energy transfer to another residue, (ii) interaction with a neighboring residue, resulting in the formation of a charge transfer complex, (iii) electron transfer from the excited state, or (iv) the presence of a cysteine residue.

However, several proteins containing more than one Trp residue are known to exhibit multiple (0,0) bands (*35*−*38*, *43*, *61*−63) arising from different Trp residues. The observation of multiple (0,0) bands is usually possible when the Trp residues in a protein are in widely different environments and photoinduced energy transfer among the emitting Trp residues is prevented.

Our previous studies on lysozyme from bacteriophage T4 and its several mutants proved that the three tryptophan residues, Trp 126, Trp 138, and Trp 158, exhibit phosphorescence (0,0) bands at 404.6, 413.6, and 407.7 nm,

Table 3: Fluorescence Lifetime Data of Wild-Type Tubulin and Its Complexes with Colchicine, AC, and Colcemid at 298 K

system	solvent	[protein] (μM)	[drug] (μM)	λ_{ex} (nm)	λ_{em} (nm)	lifetime (ns)	χ^2	τ_{av} (ns)
wild-type tubulin	PEM buffer	4	–	297	335	$\tau_1 = 4.7$ (20.8%), $\tau_2 = 1.0$ (79.2%)	1.06	1.8
	40% ethylene glycol	2	–	297	335	$\tau_1 = 5.8$ (16.5%), $\tau_2 = 1.5$ (83.5%)	1.40	2.2
tubulin–colchicine	PEM buffer	2	10	297	335	$\tau_1 = 4.1$ (15.4%), $\tau_2 = 0.4$ (84.6%)	0.74	1.0
				337	430	$\tau = 1.0$	1.35	–
	40% ethylene glycol	2	10	297	335	$\tau_1 = 5.4$ (12.4%), $\tau_2 = 1.2$ (87.6%)	0.8	1.7
				337	430	$\tau = 0.9$	1.2	–
tubulin–AC	PEM buffer	2	10	297	335	$\tau_1 = 3.9$ (18.3%), $\tau_2 = 0.3$ (81.7%)	1.02	1.0
				337	425	$\tau = 1.1$	1.25	–
	40% ethylene glycol	2	10	297	335	$\tau_1 = 5.7$ (11.4%), $\tau_2 = 1.3$ (88.6%)	1.02	1.8
				337	426	$\tau = 0.9$	0.9	
tubulin–colcemid	PEM buffer	2	10	297	335	$\tau_1 = 3.5$ (16.6%), $\tau_2 = 0.4$ (83.4%)	0.9	0.9
				337	425	$\tau = 0.9$	1.25	–
	40% ethylene glycol	2	10	297	335	$\tau_1 = 5.4$ (12.4%), $\tau_2 = 1.3$ (87.6%)	0.9	1.8
				337	425	$\tau = 0.9$	1.31	–

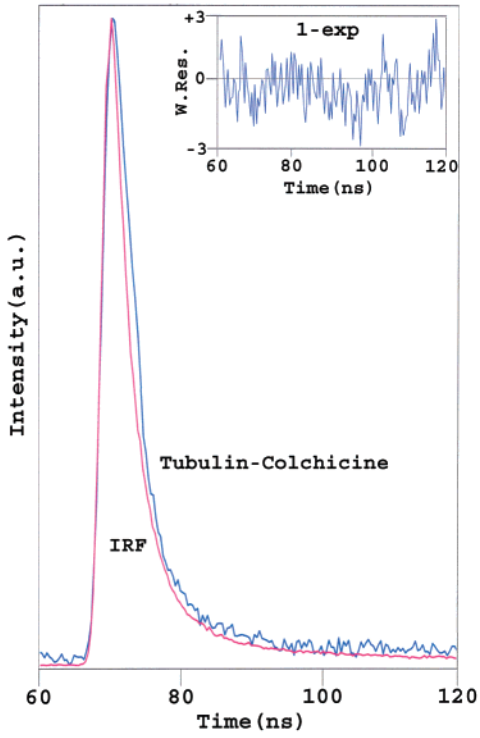

FIGURE 7: Fluorescence decay of the tubulin (2 μM)–colchicine (10 μM) complex in PEM buffer at 298 K (λ_{exc} = 337 nm, $\lambda_{monitor}$ = 430 nm, excitation band-pass = 15 nm, emission band-pass = 10 nm).

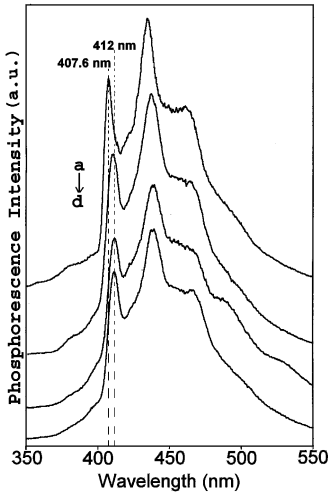

FIGURE 8: Phosphorescence spectra of wild-type tubulin (10 μM) and its complexes with different drugs in PEM buffer containing 40% ethylene glycol at 77 K: (a) wild-type tubulin, (b) tubulin with colchicine, (c) tubulin with colcemid, and (d) tubulin with AC. The concentration of the drug was 50 μM in each cases (λ_{exc} = 295 nm, excitation band-pass = 10 nm, emission band-pass = 1.5 nm).

Table 4: Phosphorescence Data of Wild-Type Tubulin (10 μM) and Its Complexes with Different Drugs (50 μM) at 77 K in 40% Ethylene Glycol Matrix

system	λ_{exc} (nm)	(0,0) band position (nm)[a]	width of the phosphorescence (0,0) band at half-maxima (cm^{-1})	phospho-rescence lifetime (s) at 77 K[b]
wild-type tubulin	295	407.6	325.0	4.4
tubulin–colchicine		412.0	365.0	4.5
tubulin–AC		412.0	355.0	4.5
tubulin–colcemid		412.2	355.0	4.5

[a] Error in the measurement of ±0.2 nm. [b] Error in the measurement of ±0.5 s.

respectively (*35*). The absolute value for the ASA (calculated using the protein coordinates taken from Protein Data Bank entry 2LYZ) are 48.45 Å^2 for Trp 126, 12.72 Å^2 for Trp 138, and 36.30 Å^2 for Trp 158. Trp 138, having the smallest ASA, exhibits the most red-shifted phosphorescence (0,0) band, while Trp 126, having the largest ASA, exhibits the most blue-shifted phosphorescence (0,0) band. The correlation of the position of the phosphorescence (0,0) band and the ASA is supported well by the crystal structure data (*64*), where Trp 138 is most buried, Trp 126 is more or less exposed, and Trp 158 is partially exposed.

In HLAD, two distinct (0,0) bands of phosphorescence appear at 406.0 and 411.0 nm. The (0,0) band at 411.0 nm corresponds to the buried Trp 314, whereas the band at 406.0 nm is assigned to Trp 15, which is more or less solvent-exposed (*61*, *62*). In our recent studies of *Escherichia coli* alkaline phosphatase (AP) (containing three Trp residues at positions 109, 220, and 268), its W220Y mutant and its Tb^{3+} complex (where two Zn^{2+} ions and one Mg^{2+} ion in wild-type protein are replaced by Tb^{3+}) reveal that Trp 109 phosphorescence appears at 414.5 nm and that of Trp 220 at 411.4 nm. The ASA values of Trp 109 are 0.68 Å^2 (in chain A) and 0.24 Å^2 (in chain B), whereas the ASA values of Trp 220 are 59.92 Å^2 (in chain A) and 83.20 Å^2 (in chain B). Trp 268 does not exhibit any phosphorescence band because of the proximity of the Cys 286–Cys 336 disulfide

bond revealed in the crystal structure of AP (*65*). Disulfides are the only known intrinsic quenchers of Trp phosphorescence in proteins (*66*). The bandwidth of the Trp 109 (0,0) band is 40 cm^{-1}, the narrowest so far observed. This Trp 109 is so far the most buried homogeneous residue (*37*) found in a protein. This is consistent with very small ASA (*37*) values of Trp 109 in both the chains. Optically detected magnetic resonance (ODMR) studies of AP (*37*) and T4 lysozyme (*36*, *37*) also support the correlation of the position of the (0,0) bands with the degree of solvent exposure.

Thus, in a given multi-Trp protein showing optically resolved (0,0) bands in its phosphorescence spectra, the positions of the (0,0) bands corresponding to different Trp residues correlate well with the degree of solvent exposure of the Trp residues.

The blue-shifted phosphorescence that is typical of free Trp in a polar solvent can be attributed to the lower polarizability of the environment and to the poor stabilization of the triplet state by a rigid solvation geometry that is organized to effectively stabilize the ground state by dipole−dipole alignment. The red-shifted (0,0) band is characteristic of a Trp residue located in a buried polarizable environment that stabilizes the triplet state more than the ground state (*42*, *57*, *67*−*69*). Apart from solvent exposure, rigidity and immediate local charges also control the position of the (0,0) band. The immediate local charge is controlled by the nature of the neighboring residues (5 Å) of Trp residues. Thus, the blue-shifted (0,0) band will correspond to a greater degree of solvent exposure with a larger ASA value and a more polar environment, while the red-shifted (0,0) band corresponds to a buried environment with a smaller ASA value and a hydrophobic polarizable environment.

Although wild-type tubulin possesses eight Trp residues (A21, A346, A388, A407, B21, B103, B346, and A407), the (0,0) band appears (at 407.6 nm) as a single peak. In the case of tubulin−drug complexes, only a single (0,0) band appears and is red-shifted (4−4.5 nm) compared to that in the free protein. The position of the (0,0) band in wild-type tubulin indicates a blue-shifted phosphorescence band characteristic of the Trp residue in a more solvent exposed and more polar environment. The red-shifted (0,0) band in the complex, on the other hand, is characteristic of a Trp residue located in a buried polarizable environment (*42*). This clearly suggests that that the binding of the drug molecule perturbs the environment of the Trp residues as revealed in our time-resolved studies.

Identification of Trp Residues Contributing to Emission. Although it is really a difficult task to identify the particular Trp residue(s) responsible for the phosphorescence, we propose a model for selecting the particular Trp residue(s) emitting in the wild-type protein and in the complex: (i) fluorescence quantum yields (ϕ_F) of wild-type tubulin and intramolecular tryptophan−tryptophan energy transfer (ET) efficiencies (Table 5), (ii) ASA values for eight Trp residues in the wild-type protein and in the complexes (Table 6), (iii) the immediate environment of each Trp residue in the wild-type protein and in the complexes determined by locating the other residues present within 5 Å of each Trp residue (Table 8) [amino acid residues common in both wild-type tubulin and the complex of tubulin with colchicine are shown in bold (Table 7)], and (iv) distances of Trp residues from rings A, B, and C of colchicine (Table 8).

The singlet−singlet nonradiative energy transfer efficiencies (E_T) using Förster's dipole−dipole ET mechanism (*70*) between tryptophyl residues are given by

$$E = \frac{{R_0}^6}{{R_0}^6 + R^6} \quad (1)$$

where R represents the Trp−Trp distance and R_0 is given by

$$R_0 = (9.79 \times 10^3)(J_{AD} n^{-4} \kappa^2 \phi_F)^{1/6} \text{ Å} \quad (2)$$

where J_{AD} denotes the spectral overlap integral, n the refractive index of the medium, κ^2 the dipole−dipole orientation factor, and ϕ_F the donor fluorescence quantum yield in the absence of accepter. κ^2 for each Trp−Trp pair is given by

$$\kappa^2 = (\cos \theta_t - \cos \theta_D \cos \theta_A)^2 \quad (3)$$

where θ_t is the angle between the donor and acceptor dipole vectors and θ_D and θ_A are the angles between the direction vector and the donor and accepter transition dipole vectors, respectively. κ^2 values were calculated for all possible combinations for the transition ($^1L_a \rightarrow {}^1L_a$, $^1L_a \rightarrow {}^1L_b$, $^1L_b \rightarrow {}^1L_a$, and $^1L_b \rightarrow {}^1L_b$) between all Trp−Trp pairs following Desie et al. (*71*) assuming the transition moment direction of ^1L_b makes an angle of 54° to the long axis of the indole molecule, while that of ^1L_a lies at an angle of −38° to the same axis (*72*).

Triplet−triplet ET between Trp residues is not possible since the distance between them is quite large (>10 Å). Intermolecular ET is also neglected since we used a micromolar concentration of protein. Taking the J_{AD} value (2.1×10^{-16} cm^6 $mmol^{-1}$) calculated for NATA in tris(hydroxymethyl)aminomethane buffer (pH 7.8) (*71*) and a refractive index (n) of 1.5 and ϕ_F for tubulin, we calculated R_0 and subsequently energy transfer efficiency (E) using eqs 2 and 1, respectively. Intramolecular Trp−Trp ET efficiency thus obtained in wild-type tubulin is presented in Table 5.

Inspection of Table 5 indicates that significant ET is possible between the following pairs: Trp B103 and Trp B407, Trp A407 and Trp B346. It is noted that Trp pairs situated at a distance greater than 20 Å are not involved in ET (Table 5A,B). The distances between different Trp residues in the complex of tubulin with colchicine have been also determined from the crystal structure data (*15*) (values given within brackets in Table 5B). The distances remain practically the same, and the calculated ET efficiencies are found to be similar to those obtained in the free protein.

The ASA values of Trp residues provided in Table 6 indicate that several Trp residues, viz., Trp A21, Trp B21, Trp B103, and Trp B346, have undergone a considerable change in ASA after formation of a complex with colchicine. The ASA values of Trp A346 in the free protein and in the complex indicate that it is exposed in both the cases (Table 6). Also, the ASA values of Trp B407 show that the residue is exposed in the free protein and in the complex. Similarly, the ASA values suggest that Trp A388 is in a buried environment both in the free protein and in the complex (Table 6). For Trp A407, the percent change in the ASA value is smaller and the ASA value increases after complex

Table 5: (A) Intramolecular Trp−Trp Energy Transfer Efficiencies in Wild-Type Tubulin[a] and (B) Inter-Trp Distances (in angstroms)[b]

(A)	A407	A21	A388	A346	B21	B103	B346	B407
				$^1L_a \rightarrow {}^1L_b$				
A407	1.00	0.00	0.01	0.00	**0.04**	0.00	0.00	0.00
A21	0.00	1.00	0.01	0.00	0.00	0.00	0.00	0.00
A388	0.00	0.01	1.00	**0.08**	0.00	0.00	**0.03**	0.00
A346	0.00	0.00	**0.08**	1.00	0.00	0.00	0.00	0.00
B21	**0.04**	0.00	0.00	0.00	1.00	0.01	0.00	0.00
B103	0.00	0.00	0.00	0.00	0.01	1.00	0.00	**0.27**
B346	0.00	0.00	**0.03**	0.00	0.00	0.00	1.00	0.00
B407	0.00	0.00	0.00	0.00	0.00	**0.27**	0.00	1.00
				$^1L_a \rightarrow {}^1L_b$				
A407	1.00	0.00	0.00	0.00	0.00	0.03	**0.18**	0.00
A21	0.00	1.00	0.01	0.00	0.00	0.00	0.00	0.00
A388	0.00	0.01	1.00	0.00	0.00	0.00	0.00	0.00
A346	0.00	0.00	0.00	1.00	0.00	0.00	0.00	0.00
B21	0.00	0.00	0.00	0.00	1.00	0.00	0.00	0.00
B103	0.03	0.00	0.00	0.00	0.00	1.00	0.00	0.02
B346	**0.18**	0.00	0.00	0.00	0.00	0.00	1.00	0.00
B407	0.00	0.00	0.00	0.00	0.00	0.02	0.00	1.00
				$^1L_b \rightarrow {}^1L_a$				
A407	1.00	0.00	0.01	0.00	0.00	0.01	0.00	0.00
A21	0.00	1.00	0.00	0.00	0.00	0.00	0.00	0.00
A388	0.01	0.00	1.00	0.08	0.00	0.00	0.00	0.00
A346	0.00	0.00	**0.08**	1.00	0.00	0.00	0.00	0.00
B21	0.00	0.00	0.00	0.00	1.00	0.00	0.00	0.00
B103	0.01	0.00	0.00	0.00	0.00	1.00	0.01	**0.18**
B346	0.00	0.00	0.00	0.00	0.00	0.01	1.00	0.00
B407	0.00	0.00	0.00	0.00	0.00	**0.18**	0.00	1.00
				$^1L_a \rightarrow {}^1L_a$				
A407	1.00	0.00	0.00	0.00	0.01	0.00	**0.14**	0.00
A21	0.00	1.00	**0.03**	0.00	0.00	0.00	0.00	0.00
A388	0.00	**0.03**	1.00	0.01	0.00	0.01	**0.05**	0.00
A346	0.00	0.00	0.01	1.00	0.00	0.00	0.00	0.00
B21	0.01	0.00	0.00	0.00	1.00	**0.07**	0.00	0.00
B103	0.00	0.00	0.01	0.00	**0.07**	1.00	0.00	0.01
B346	**0.14**	0.00	**0.05**	0.00	0.00	0.00	1.00	0.00
B407	0.00	0.00	0.00	0.00	0.00	0.01	0.00	1.00

(B)	A407	A21	A388	A346	B21	B103	B346	B407
A407	−	33.60 (35.28)[c]	26.11 (26.11)[c]	42.94 (44.26)[c]	24.48 (26.68)[c]	24.49 (25.54)[c]	**15.32 (16.06)**[c]	40.24 (40.86)[c]
A21	33.60 (35.28)[c]	−	26.53 (26.47)[c]	34.73 (36.05)[c]	39.78 (44.30)[c]	55.34 (58.63)[c]	40.86 (43.32)[c]	70.03 (72.97)[c]
A388	26.11 (26.11)[c]	26.53 (26.47)[c]	−	**17.21 (18.73)**[c]	45.73 (47.86)[c]	49.87 (51.78)[c]	23.80 (24.78)[c]	64.99 (66.62)[c]
A346	42.94 (44.26)[c]	34.73 (36.05)[c]	**17.21 (18.73)**[c]	−	62.39 (66.37)[c]	66.66 (69.80)[c]	39.49 (41.04)[c]	81.82 (83.83)[c]
B21	24.48 (26.88)[c]	39.78 (44.30)[c]	45.73 (47.86)[c]	62.39 (66.37)[c]	−	24.35 (24.83)[c]	34.89 (36.87)[c]	34.22 (34.56)[c]
B103	24.49 (25.54)[c]	55.34 (58.63)[c]	49.87 (51.78)[c]	66.66 (69.80)[c]	24.35 (24.83)[c]	−	30.30 (32.85)[c]	**16.18 (15.04)**[c]
B346	**15.32 (16.06)**[c]	40.86 (43.32)[c]	23.80 (24.78)[c]	39.49 (41.04)[c]	34.89 (36.87)[c]	30.30 (32.85)[c]	−	43.64 (45.13)[c]
B407	40.24 (40.86)[c]	70.03 (72.97)[c]	64.99 (66.62)[c]	81.82 (83.83)[c]	34.22 (34.56)[c]	**16.18 (15.04)**[c]	43.64 (45.13)[c]	−

[a] Values are listed for the $^1L_a \rightarrow {}^1L_a$, $^1L_a \rightarrow {}^1L_b$, $^1L_b \rightarrow {}^1L_a$, and $^1L_a \rightarrow {}^1L_a$ transitions. [b] From the center of mass of the adjacent double bond of the nitrogen atom of the indole moiety of tryptophan residues. [c] Values in parentheses are the Trp−Trp distances in the crystal structure of the colchicine−tubulin complex (PDB entry 1SA0).

Table 6: Accessible Surface Areas (in square angstroms) for Each Trp Residue in Wild-Type Tubulin (PDB entry 1TUB) and Its Complex with Colchicine (PDB entry 1SA0)

residue	ASA for wild-type tubulin (Å^2)	ASA for the tubulin−colchicine complex (Å^2)	change in ASA (Å^2)
Trp A21	17.46	4.48	−12.98
Trp A346	84.75	88.17	3.42
Trp A388	0.83	0.06	−0.77
Trp A407	32.93	42.07	9.14
Trp B21	33.17	1.70	−31.47
Trp B103	9.28	2.83	−6.45
Trp B346	15.06	5.54	−9.52
Trp B407	165.72	144.93	−20.79

formation. The ASA values of Trp B103 are also indicative of a buried residue in both the free protein and the complex.

The fluorescence quantum yield (ϕ_F) for pure tryptophan is 0.14 (*73*). The observed ϕ_F for wild-type tubulin is 0.06. Since tubulin contains eight Trp residues, the ϕ_F value indicates that at least three or four Trp residues are contributing to emission of the free protein. This is based on the assumption that the fluorescence of these Trp residues is not appreciably quenched due to the presence of other nearby residues. Since the phosphorescence (0,0) band in the free protein appears at 407.6 nm, the Trps contributing to the emission should be solvent-exposed and have polar environments. Thus, the comparatively solvent exposed residues, viz., Trp A346, Trp A407, Trp B21, and Trp B407, having different polar residues within 5 Å (Table 7) are likely candidates for contributing to the emission of the free protein. The possibility of the contribution from Trp A388 is eliminated since it is the most buried residue.

Table 7: Tryptophan Neighbors in Tubulin (PDB entry 1TUB) and the Colchicine−Tubulin Complex (PDB entry 1SA0) within 5 Å[a]

system	A21	A346	A388	A407	B21	B103	B346	B407
wild-type tubulin	**Ser A6** (p) **His A8** (p) **Gly A17** **Asn A18** (p) **Cys A20** (p) **Glu A22** (p) **Leu A23** **Tyr A24** (p) **Ala A65** **Phe A67**	**Tyr A262** (p) **Met A313** **Val A344** **Asp A345** (p) **Cys A347** (p) **Val A435**	Tyr A172 (p) **Phe A267** **Ile A384** **Ala A385** **Ala A387** **Ala A389** **Met A425** **Leu A428** **Tyr A432** (p)	**His A406** (p) **Tyr A408** (p) Ile B165 Asp B199 (p) **Ala B256** **Val B257** **Val B260**	**His B6** (p) **Gln B8** (p) **Gly B17** **Phe B20** **Glu B22** (p) Ile B24 Ile B30 Arg B64 (p) **Ala B65**	**Asn B102** (p) **Ala B104** **His B107** (p) Tyr B108 (p) Gly B144 **Ser B147** (p) **Gly B148** Met B149 **Thr B15** (p) Tyr B185 (p) **Thr B18** (p) **Leu B189** Met B413	**Leu A397** Arg A402 (p) Leu B313 **Val B344** **Glu B345** (p) **Ile B347** **Tyr B435** (p)	**Asn B102** (p) **Leu B405** **His B406** (p) **Tyr B408** (p)
colchicine−tubulin	**Ser A6** (p) **His A8** (p) **Gly A17** **Asn A18** (p) Ala A19 **Cys A20** (p) **Glu A22** (p) **Leu A23** **Tyr A24** (p) Cys A25 (p) Phe A52 Phe A53 Pro A63 Arg A64 (p) **Ala A65** **Phe A67** Phe A87	Pro A261 **Tyr A262** (p) **Met A313** **Val A344** **Asp A345** (p) **Cys A347** (p) Pro A348 **Val A435**	Met A203 **Phe A267** **Ile A384** **Ala A385** **Ala A387** **Ala A389** **Met A425** **Leu A428** **Tyr A432** (p)	Phe A404 **His A406** (p) **Tyr A408** (p) **Ala B256** **Val B257** **Val B260**	**His B6** (p) **Gln B8** (p) **Gly B17** Ala B18 **Phe B20** **Glu B22** (p) Pro B63 **Ala B65** Phe B87	**Asn B102** (p) **Ala B104** **His B107** (p) **Ser B147** (p) **Gly B148** **Thr B151** (p) Asn B186 (p) Ser B190 (p) Gln B193 (p)	**Leu A397** Lys A401 (p) Arg B311 (p) **Val B344** **Glu B345** (p) **Ile B347** **Tyr B435** (p) Asp B437 (p) Ala B438	**Asn B102** (p) Phe B404 **Leu B405** **His B406** (p) **Tyr B408** (p) Thr B409 (p) Gly B410 Glu B411

[a] The distances are from the center of the indole moiety of the Trp residues. Bold amino acid residues are common to both wild-type tubulin and its complex with colchicine. A lowercase p in parentheses denotes a polar residue.

It is noted from Table 7 that residues Ile B24, Ile B30, and Arg B64 are within 5 Å of Trp B21, while in the complex, Ala B18, Pro B63, Ala B65, and Phe B87 are within 5 Å of Trp B21. The common neighboring residues of Trp B21 in the protein and in the complex are shown as bold letters in Table 7. Displacement of polar residue Arg B64 from Trp B21 and the presence of Ala B18, Pro B63, Ala B65, and Phe B87 within 5 Å of Trp B21 suggest that Trp B21 moves from a more polar to a more hydrophobic (less polar) environment after complex formation. The presence of an Arg residue near a Trp residue could increase the polarity of the Trp environment due to the charge of the Arg side chain, the formation of a hydrogen bond of one of the NH groups on the Arg side chain with the indole ring, or the interaction through a NH$-\pi$ bond with the indole ring (*74*−*78*). Thus, Trp B21 moves from a more polar and solvent exposed environment to a more hydrophobic and buried environment (Table 7). This clearly implies that Trp B21 contributes to the emission of the free protein as well as the complex.

A similar comparison for immediate residues of Trp B346 from Table 7 shows that Trp B346 is moving from a less polar to a more polar environment. Trp B346 has five polar residues within 5 Å in the complex compared to three polar residues in wild-type tubulin (Table 7). Although Arg A402 is somewhat removed from Trp B346 in the complex, Arg B311 moves closer in the complex. Lys A401 and Asp B437 present within 5 Å of Trp B346 make the environment of Trp B346 more polar in the complex. Trp A21 also moves from a less polar to a more polar environment. Trp A21 has eight polar residues within 5 Å in the complex compared to six polar residues in the wild-type protein (Table 7).

Trp B346 and Trp B103, having small ASA values and being involved in intramolecular ET to Trp A407 and Trp B407, respectively (Table 6), could be considered not to contribute to the emission of the free protein. Although Trp A21 and Trp B346 exhibited a substantial decrease in ASA after complex formation, the immediate environment of Trp A21 and Trp B346 in the complex as discussed is not favorable for the observed shift of phosphorescence.

Trp A346 and Trp B407 are found to be solvent-exposed both in the wild type and in the complex. Thus, although these two residues contribute to the emission of the free protein, they are possibly quenched in the complex. Since Trp A407 exhibits a larger ASA in the complex and is the closest to all three rings of colchicine (Table 8), Trp A407 could also be considered nonemissive in the complex. Thus, in the complex, Trp B21, Trp B346, Trp B103, and Trp A21 should contribute if one considers only the ASA values in the free protein and in the complex. However, Trp A21 and Trp B346 as discussed earlier, moving to a more polar environment in the complex (more polar residues within 5 Å in the complex), could be eliminated. As a result, Trp B21 and Trp B103 should contribute to the emission in the complex.

Our results showing a shift of the (0,0) band of phosphorescence from a more polar and more solvent exposed environment to a less polar and more buried region clearly indicate that mainly Trp A346, Trp A407, Trp B21, and Trp B407 contribute to the emission of the protein while Trp B21 and Trp B103 contribute to the emission of the complex on the basis of the ASA value, immediate environments, the ET efficiency, and the distance of the Trp residues from the drug molecule.

Table 8: Distances[a] from Different Moieties of Colchicine to Different Tryptophan Residues in the Crystal Structure of the Colchicine−Tubulin Complex (PDB entry 1SA0)

position (Trp residue)	distance from ring A (Å)	distance from ring B (Å)	distance from ring C (Å)
A21	30.4	28.82	30.28
A346	48.45	46.20	44.81
A388	29.79	27.29	25.83
A407	14.25	13.02	12.39
B21	20.83	23.19	25.11
B103	30.58	32.03	32.31
B346	21.74	20.51	17.85
B407	42.31	43.93	44.02

[a] From the center of mass of the adjacent double bond of the nitrogen atom of the indole moiety of the tryptophan residue to the center of mass of rings A, B, and C of the colchicine molecule.

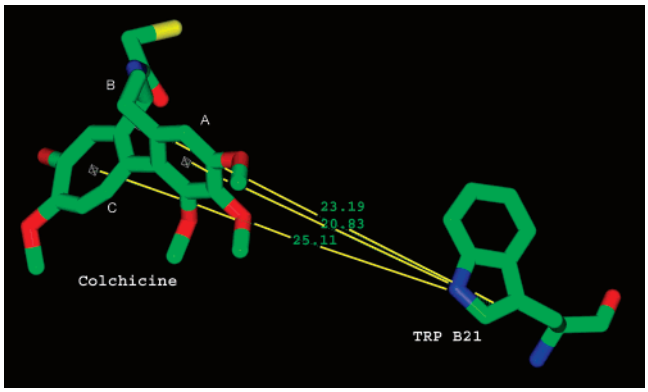

FIGURE 9: Colchicine and Trp B21 molecule viewed in stick representation. The distance represented here is between the center of mass of rings A, B, and C of the colchicine molecule and the center of mass of the double bond of the adjacent nitrogen atom of the indole moiety of Trp B21. This figure was generated from the tubulin−colchicine complex crystal structure (PDB entry 1SA0) using Insight II (Biosym/MSI).

Similar results for time-resolved fluorescence at room temperature and phosphorescence at 77 K observed in the case of the complexes of tubulin with the analogues colcemid and AC imply a similar prediction regarding the contribution of the Trp emission as interpreted in the tubulin−colchicine complex.

The width of the phosphorescence (0,0) band reflects the heterogeneity of the Trp environment (*37*) in a protein. The most homogeneous environment so far observed in a protein is for Trp 109 in AP from *E. coli* (*37*). Trp 109 in AP exhibits a bandwidth of 40 cm^{-1} (*37*) indicative of a quasi-crystalline environment. Table 4 indicates that the bandwidth of the (0,0) band in the wild type changes from 325 to ∼350−360 cm^{-1} in the complexes of tubulin and colchicine, AC, and colcemid. This implies that the emitting Trp residues in the complex move to a somewhat less homogeneous environment compared to that in the free protein.

The lifetimes of the phosphorescence of tryptophan residues in tubulin and the complexes with the drugs have also been measured at 77 K (Table 4). The lifetime values observed are similar for the wild-type protein and its complexes. The lifetime is found to be somewhat smaller than typical lifetime values (5−6 s) observed for Trp residues in proteins (*34*).

Energy Transfer (ET) from Trp Residues of Tubulin to Drug Molecules. The quantum yields of the Trp residues in the complexes were also measured (Table 1) and found to be lower than that of pure tubulin, indicating either static quenching due to the binding of the drug molecules, ET from Trp residues to the drug molecules, or both. However, the shortening of the lifetime of Trp fluorescence in the complexes (Table 3) suggests an additional nonradiative channel for the fluorescence state of Trp residues operating in the complexes. This aspect and also the excitation spectra monitoring the drug emission (inset of Figure 4) imply ET from Trp residues to drug molecules. The ET from the Trp residues to colchicine in tubulin colchicine complex had been addressed by Bhattacharyya et al. (*32*). Comparison of the absorption spectra and the excitation spectra and the quenching studies of Trps in the complex in the absence and presence of acrylamide (*32*) indicated that the two inaccessible Trp residues acted as donors in the ET process. This was also supported by REES studies (*31*).

Singlet−singlet nonradiative ET depends not only on the distance between the donor (D) and the acceptor (A) but also on the orientation of D with respect to A (*35*, *43*, *70*). Although the transition dipole moment direction of Trp is well-known, that in colchicine is not known. Thus, it is difficult to identify the particular Trp residues involved in the ET process. However, from the distances of Trp residues from rings A, B, and C of colchicine and the ASA values of Trp residues, a tentative prediction could be made. Although the residue Trp A407 is the nearest to colchicine (Table 8), its ASA is quite large (Table 6), and thus, it is unlikely to assume Trp A407 as the donor according to ref *32*. According to the ASA values, the two inaccessible Trp residues could be Trp A388 and Trp B103; however, their distances from the colchicine rings (∼30 Å) make them less probable candidates for acting as donors in the ET process. Thus, Trp B21 and Trp B346 which are ∼20 Å from the colchicine rings could be the possible donors in the ET process. In that case, the ET efficiency (E_T) could be estimated from the reduction of the average lifetime (τ_{av}) (Table 3) in the complex (*73*). This argument provides an E_T [$=1 - \langle\tau_{DA}\rangle/\langle\tau_D\rangle$] of 0.44 and the rate constant of energy transfer, k_{ET} (4.4×10^8 s^{-1}), where $\langle\tau_D\rangle$ and $\langle\tau_{DA}\rangle$ are the average lifetime of wild-type tubulin and the tubulin−drug complexes, respectively (Table 3). Calculation of E_T from the steady state emission is not applicable since static quenching is also taking place in the complex.

CONCLUSION

Time-resolved fluorescence and phosphorescence studies indicate that the emitting Trp residue is pushed toward a hydrophobic region due to complex formation. The environment is somewhat heterogeneous in the complex compared to that in the wild-type protein. The analysis of the ASA values, the nature of the residues present near Trp residues (<5 Å) in wild-type tubulin and in the complex of tubulin with colchicine, AC, and colcemid, and the inter-Trp−Trp ET efficiency indicate that Trp A346, Trp A407, Trp B21, and Trp B407 contribute mainly to the emission of free tubulin while Trp B21 and Trp B103 are the major contributors to the emission of the complex. The distances of the indole moiety of the Trp residues from rings A, B, and C of the colchicine molecule also support the view. Trp A346 and Trp B407 are shown to be quenched in the complex from the ASA values and the immediate environments. Trp

A407 which is closest to colchicine rings A, B, and C is also supposed to be quenched. The analysis of the results suggests a methodology for identifying the perturbed Trp residues in a multi-tryptophan protein−drug complex without performing Trp mutation. The average lifetime of fluorescence of Trp residues in tubulin and its complex with colchicine, the distance of Trp residues from the colchicine, and the ASA values of Trp residues are employed to shed light on the ET from Trp residues to colchicine in the complex.

ACKNOWLEDGMENT

We gratefully acknowledge Prof. B. Bhattacharyya for providing the protein tubulin and the drugs colchicine and AC. AC was a kind gift of T. J. Fitzgerald (Florida A & M University). We acknowledge Subhodip Samanta for assistance in the calculations. We are grateful to the reviewers for their helpful and constructive suggestions.

REFERENCES

1. Dustin, P. (1979) Microtubules and mitosis, *Bull. Assoc. Anat. (Nancy) 63*, 109−126.
2. Avila, J. (1990) Microtubule dynamics; Review, *FASEB J. 4*, 3284−3290.
3. Olmsted, J. B., and Borisy, G. G. (1973) Microtubules, *Annu. Rev. Biochem. 42*, 507−540.
4. Brossi, A., Yeh, H. J., Chrzanowska, M., Wolff, J., Hamel, E., Lin, C. M., Quin, F., Sulfness, M., and Silverton, J. (1988) Colchicine and its analogues. Recent findings, *Med. Res. Rev. 8*, 77−94.
5. Wallace, S. L. (1974) Colchicine, *Semin. Arthritis Rheum. 3*, 369−381.
6. Malkinson, F. D. (1982) Colchicine: New use of an old, old drug, *Arch. Dermatol. 118*, 453−457.
7. Hillmann, G., and Ruthmann, A. (1982) Effect of mitotic inhibitors on the ultra structure of root meristem cells, *Planta 155*, 124−132.
8. Nakagawa, Y., Nakamura, S., Kase, Y., Noguehi, T., and Ishihara, T. (1987) Colchicine lesions in the rat hippocampus mimic the alterations of several markers of Alzheimer's disease, *Brain Res. 408*, 57−64.
9. Mattson, M. P. (1992) Effects of microtubule stabilization and destabilization on tau immunoreactivity in cultured hippocampal neurons, *Brain Res. 582*, 107−118.
10. Olmsted, J. B., and Borisy, G. G. (1973) Characterization of microtubule assembly in porcine brain extracts by viscometry, *Biochemistry 12*, 4282−4289.
11. Nunez, J., Fellous, A., Francon, J., and Lennon, A. M. (1979) Competitive inhibition of colchicine binding to tubulin by microtubule-associated proteins, *Proc. Natl. Acad. Sci. U.S.A. 76*, 86−90.
12. Mundy, W. R., and Tilson, H. A. (1990) Neurotoxic effects of colchicines, *Neurotoxicology 11*, 539−547.
13. Newell, D. W., Hsu, S. S., Papermaster, V., and Malouf, A. T. (1993) Colchicine is selectively neurotoxic to dentate granule cells in organotypic cultures of rat hippocampus, *Neurotoxicology 14*, 375−380.
14. Arai, T., and Okuyama, T. (1973) Purification and properties of colchicine-binding protein from the bovine brain, *Seikagaku 45*, 19−29.
15. Ravelli, R. B. G., Gigant, B., Curmi, P. A., Jourdain, I., Lachkar, S., Sobel, A., and Knossow, M. (2004) Insight into tubulin regulation from a complex with colchicine and a stathmin-like domain, *Nature 428*, 198−202.
16. Bhattacharyya, B., and Wolff, J. (1974) Promotion of fluorescence upon binding of colchicine to tubulin, *Proc. Natl. Acad. Sci. U.S.A. 71*, 2627−2631.
17. Wilson, L., and Bryan, J. (1974) Biochemical and pharmacological properties of the microtubules, *Adv. Cell Mol. Biol. 3*, 21−72.
18. Dustin, P. (1978) *Microtubules*, Springer-Verlag, New York.
19. Timasheff, S. N., and Grisham, L. M. (1980) In vitro assembly of cytoplasmic microtubules, *Annu. Rev. Biochem. 49*, 565−591.
20. Margolis, R. L., and Wilson, L. (1981) Microtubule treadmills: Possible molecular machinery, *Nature 293*, 705−711.
21. Bhattacharyya, B., and Wolff, J. (1974) Thyroid tubulin: Purification and properties, *Biochemistry 13*, 2364−2369.
22. Detrich, H. W., III, Williams, R. C., Jr., Macdonald, T. L., Wilson, L., and Puett, D. (1981) Changes in the circular dichroic spectrum of colchicine associated with its binding to tubulin, *Biochemistry 20*, 5999−6005.
23. Garland, D. L. (1978) Kinetics and mechanism of colchicines binding to tubulin: Evidence for ligand-induced conformational changes, *Biochemistry 17*, 4266−4272.
24. Lambeir, A., and Engelborghs, Y. (1981) A fluorescence stopped flow study of colchicine binding to tubulin, *J. Biol. Chem. 256*, 3279−3282.
25. Fitzgerald, T. J. (1976) Molecular features of colchicines associated with antimitotic activity and inhibition of tubulin polymerization, *Biochem. Pharmacol. 25*, 1383−1387.
26. Ray, K., Bhattacharyya, B., and Biswas, B. B. (1981) Role of B-ring of colchicine in its binding to tubulin, *J. Biol. Chem. 256*, 6241−6244.
27. Hastie, S. B., Puett, D., Macdonald, T. L., and Williams, R. C., Jr. (1984) Binding of tubulin of the colchicine analog 2-methoxy-5-(2′,3′,4′-trimethoxyphenyl)tropone: Thermodynamic and kinetic aspect, *J. Biol. Chem. 259*, 7391−7398.
28. Biswas, B. B., Sen, K., Ghosh Chodhury, G., and Bhattacharyya, B. (1984) Molecular biology of tubulin: Its interaction with drugs and genomic organization, *J. Biosci. 6*, 431−457.
29. Chakrabarti, G., Sengupta, S., and Bhattacharyya, B. (1996) Thermodynamics of colchicinoid-tubulin interactions. Role of B-ring and C-7 substituent, *J. Biol. Chem. 271*, 2897−2901.
30. Pyles, E. A., Rava, R. P., and Hastie, S. B. (1992) Effect of B-ring substituents on absorption and circular dichroic spectra of colchicine analogues, *Biochemistry 31*, 2034−2039.
31. Guha, S., Rawat, S. S., Chattopadhyay, A., and Bhattacharyya, B. (1996) Tubulin conformation and dynamics: A red edge excitation shift study, *Biochemistry 35*, 13426−13433.
32. Bhattacharyya, A., Bhattacharyya, B., and Roy, S. A. (1993) Study of colchicine tubulin complex by donor quenching of fluorescence energy transfer, *Eur. J. Biochem. 299*, 757−761.
33. Royer, C. A., Gardner, J. A., Beechem, J. M., Brochon, J. C., and Matthews, K. S. (1990) Resolution of the fluorescence decay of the two tryptophan residues of lac repressor using single tryptophan mutants, *Biophys. J. 58*, 363−378.
34. Maki, A. H. (1984) in *Biological Magnetic Resonance* (Berliner, L. J., and Reuben, J., Eds.) Vol. 6, pp 187−294, Plenum Press, New York.
35. Ghosh, S., Zang, L. H., and Maki, A. H. (1988) Relative efficiency of long range nonradiative energy transfer among tryptophan residues in bacteriophage T4 lysozyme, *J. Chem. Phys. 88*, 2769−2775.
36. Ghosh, S., Zang, L. H., and Maki, A. H. (1988) Optically detected magnetic resonance study of tyrosine residues in point-mutated bacteriophage T4 lysozyme, *Biochemistry 27*, 7816−7820.
37. Ghosh, S., Misra, A., Ozarowski, A., Stuart, C., and Maki, A. H. (2001) Characterization of the tryptophan residues of *Escherechia coli* alkaline phosphatase by phosphorescence and optically detected magnetic resonance spectroscopy, *Biochemistry 40*, 15024−15030.
38. Ghosh, S., Misra, A., Ozarowski, A., and Maki, A. H. (2003) Low-temperature study of photoinduced energy transfer from tryptophan residues of *Escherichia coli* alkaline phosphatase to bound terbium, *J. Phys. Chem. B 107*, 11520−11526.
39. Hahn, D. K., and Callis, P. R. (1997) Lowest triplet state of indole: An ab initio study, *J. Phys. Chem. A 101*, 2686−2691.
40. Galley, W. C., and Purkey, R. M. (1970) Role of Heterogeneity of the Solvation Site in Electronic Spectra in Solution, *Proc. Natl. Acad. Sci. U.S.A. 67*, 1116−1121.
41. Hershberger, M. V., Maki, A. H., and Galley, W. C. (1980) Phosphorescence and optically detected magnetic resonance studies of a class of anomalous tryptophan residues in globular proteins, *Biochemistry 19*, 2204−2209.
42. Ozarowski, A., Barry, J. K., Matthews, K. S., and Maki, A. H. (1999) Ligand-induced conformational changes in lactose repressor: A phosphorescence and ODMR study of single-tryptophan mutants, *Biochemistry 38*, 6715−6722.
43. Saha Sardar, P., Maity, S. S., Ghosh, S., Chatterjee, J., Maiti, T. K., and Dasgupta, S. (2006) Characterization of the tryptophan residues of human placental ribonuclease inhibitor (hRI) and its complex with bovine pancreatic ribonuclease A (RNase A) by

steady state and time resolved emission spectroscopy, *J. Phys. Chem. B 110*, 21349−21356.
44. Hamel, E., and Lin, C. (1981) Glutamate-induced polymerization of tubulin: Characteristics of the reaction and application to the large-scale purification of tubulin, *Arch. Biochem. Biophys. 209*, 29−40.
45. Lowry, O. H., Rosenbrough, N. J., Farr, A. I., and Randall, R. J. (1951) Protein measurement with the Folin phenol reagent, *J. Biol. Chem. 193*, 265−275.
46. Nogales, E., Wolf, S. G., and Downing, K. H. (1998) Structure of the $\alpha\beta$ tubulin dimer by electron crystallography, *Nature 391*, 199−203.
47. Hubbard, S. J., and Thornton, J. M. (1993) *NACCESS*, Computer Program Department of Biochemistry and Molecular Biology, University College London, London.
48. Demas, J. N., and Crosby, G. A. (1971) The measurement of photoluminescence quantum yields. A review, *J. Phys. Chem. 75*, 991−1025.
49. Chen, R. F. (1967) Fluorescence quantum yields of tryptophan and tyrosine, *Anal. Lett. 1*, 35−42.
50. Bhattacharyya, B., and Wolff, J. (1984) Immobilization-dependant fluorescence of colchicine, *J. Biol. Chem. 259*, 11836−11843.
51. Lakowicz, J. R., and Cherek, H. (1981) Resolution of heterogeneous fluorescence from proteins and aromatic amino acids by phase-sensitive detection of fluorescence, *J. Biol. Chem. 256*, 6348−6353.
52. Lakowicz, J. R., and Balter, A. (1982) Direct recording of the initially excited and the solvent relaxed fluorescence emission spectra of tryptophan by phase sensitive detection of fluorescence, *Photochem. Photobiol. 36*, 125−132.
53. Lakowicz, J. R., and Balter, A. (1982) Resolution of initially excited and relaxed states of tryptophan fluorescence by differential-wavelength deconvolution of time-resolved fluorescence decays, *Biophys. Chem. 15*, 353−360.
54. Szabo, A. G., and Rayner, D. M. (1980) Fluorescence decay of tryptophan conformers in aqueous solution, *J. Am. Chem. Soc. 102*, 554−563.
55. Callis, P. R., and Vivian, J. T. (2003) Understanding the variable fluorescence quantum yield of tryptophan in proteins using QM-MM simulations. Quenching by charge transfer to the peptide backbone, *Chem. Phys. Lett. 369*, 409−414.
56. Willets, K. A., Callis, P. R., and Moerner, W. E. (2004) Experimental and theoretical investigations of environmentally sensitive single-molecule fluorophores, *J. Phys. Chem. B 108*, 10465−10473.
57. Callis, P. R., and Liu, T. (2004) Quantitative predictions of fluorescence quantum yields for tryptophan in proteins, *J. Phys. Chem. B 108*, 4248−4259.
58. Kurz, L. C., Fite, B., Jean, J., Park, J., Erpelding, T., and Callis, P. R. (2005) Photophysics of tryptophan fluorescence: Link with the catalytic strategy of the citrate synthase from *Thermoplasma acidophilum*, *Biochemistry 44*, 1394−1413.
59. Liu, T., Callis, P. R., Hesp, B. H., de Groot, M., Buma, W. J., and Broos, J. (2005) Ionization potentials of fluoroindoles and the origin of non-exponential tryptophan fluorescence decay in proteins, *J. Am. Chem. Soc. 127*, 4104−4113.
60. Ide, G., and Engelborghs, Y. (1981) Fluorescence quenching and induced dissociation of the tubulin-colchicine complex by iodide, *J. Biol. Chem. 256*, 11684−11687.
61. Eftink, M. R. (1992) in *Advances in Biophysical Chemistry* (Bush, C. A., Ed.) Vol. 2, pp 81−114, JAI Press, Greenwich, CT.
62. Purkey, R. M., and Galley, W. C. (1970) Phosphorescence studies of environmental heterogeneity for tryptophyl residues in proteins, *Biochemistry 9*, 3569−3575.
63. Eftink, M. R., Ramsay, G. D., Burns, L., Maki, A. H., Mann, C. J., Matthews, C. R., and Ghiron, C. A. (1993) Luminescence studies with Trp repressor and its single-tryptophan mutants, *Biochemistry 32*, 9189−9198.
64. Remington, S. J., Anderson, W. F., Owen, J., Ten Eyck, L. F., Grainger, C. T., and Matthews, B. W. (1978) Structure of the lysozyme from bacteriophage T4: An electron density map at 2.4 Å resolution, *J. Mol. Biol. 118*, 81−98.
65. Stee, B., Holtz, K. M., and Kantrowitz, E. R. (2000) A revised mechanism for the alkaline phosphatase reaction involving three metal ions, *J. Mol. Biol. 299*, 1323−1331.
66. Li, Z., and Galley, W. C. (1989) Evidence for ligand-induced conformational changes in proteins from phosphorescence spectroscopy, *Biophys. J. 56*, 353−360.
67. Lam, W. C., Maki, A. H., Itoh, T., and Hakoshima, T. (1992) Phosphorescence and optically detected magnetic resonance measurements of the 2′AMP and 2′GMP complexes of a mutant ribonuclease T1 (Y45W) in solution: Correlation with X-ray crystal structures, *Biochemistry 31*, 6756−6760.
68. Von Shutz, J. U., Zuclich, J. A., and Maki, A. H. (1974) Resolution of tryptophan phosphorescence from multiple sites in proteins using optical detection of magnetic resonance, *J. Am. Chem. Soc. 96*, 714−718.
69. Kwiram, A. L., and Ross, J. B. A. (1982) Optical detection of magnetic resonance in biologically important molecules, *Annu. Rev. Biophys. Bioeng. 11*, 223−249.
70. Förster, T. (1948) Zwischenmolekulare energiewanderung und fluoreszenz, *Ann. Phys. (Weinheim, Ger.) 2*, 55−75. Förster, T. (1959) 10th Spiers Memorial Lecture. Transfer mechanisms of electronic excitation, *Discuss. Faraday Soc. 27*, 7−17.
71. Desie, G., Boens, N., and De Schryver, F. C. (1986) Study of the time-resolved tryptophan fluorescence of crystalline α-chymotrypsin, *Biochemistry 25*, 8301−8308.
72. Yamamoto, Y., and Tanaka, J. (1972) Polarised absorption spectra of crystals of indole and its related compounds, *Bull. Chem. Soc. Jpn. 45*, 1362−1366.
73. Lakowicz, J. R. (1999) *Principles of Fluorescence Spectroscopy*, Chapter 17, Kluwer/Plenum Press, New York.
74. Samanta, U., Pal, D., and Chakrabarti, P. (2000) Environment of tryptophan side chains in proteins, *Proteins 38*, 288−300.
75. Nanda, V., and Brand, L. (2000) Aromatic interactions in homeodomains contribute to the low quantum yield of a conserved, buried tryptophan, *Proteins: Struct., Funct., Genet. 40*, 112−125.
76. Vivian, J. T., and Callis, P. R. (2001) Mechanisms of tryptophan fluorescence shifts in proteins, *Biophys. J. 80*, 2093−2109.
77. Koenig, S., Muller, L., and Smith, D. K. (2001) Dendritic biomimicry: Microenvironmental hydrogen-bonding effects on tryptophan fluorescence, *Chem.—Eur. J. 7*, 979−986.
78. Harvey, B. J., Bell, E., and Brancaleon, L. (2007) A tryptophan rotamer located in a polar environment probes pH-dependent conformational changes in bovine β-lactoglobulin A, *J. Phys. Chem. B 111*, 2610−2620.

BI701412K